Dislocations stopped by the $\Sigma = 9$ (122) grain boundary in Si. An HREM study of thermal activation

J. Thibault-Desseaux, J.L. Putaux, A. Bourret, H.O.K. Kirchner

J. Phys. France **50** (1989) 2525-2540 15 SEPTEMBRE **1989,** PAGE 2525

Classification
Physics Abstracts
61.70G, J, L, N, P, Y

Dislocations stopped by the $\Sigma = 9(122)$ grain boundary in Si. An HREM study of thermal activation

J. Thibault-Desseaux ([1]), J. L. Putaux ([1]), A. Bourret ([1]) and H. O. K. Kirchner ([2])

([1]) Département de Recherche Fondamentale, Service de Physique, Centre d'Etudes Nucléaires, 85X, 38041 Grenoble Cedex, France
([2]) Institut für Festkörperphysik, Universität Wien, A-1090 Boltzmanngasse 5, Vienna, Austria

(*Reçu le 17 mars 1989, accepté sous forme définitive le 3 mai 1989*)

Résumé. — Les configurations des dislocations résiduelles, observées après l'intégration dans le joint de grains des dislocations glissiles, sont expliquées par analogie avec le glissement dévié dans le massif. Les dissociations, cristallographiquement possibles, des dislocations du grain en dislocations parfaites ou imparfaites du réseau DSC sont discutées. Les configurations les plus favorables énergétiquement servent d'étapes intermédiaires lors de l'activation thermique qui fait intervenir à la fois le glissement et la montée. L'activation thermique bloque au joint les dislocations à 60°, alors qu'elle aide les dislocations vis à le traverser.

Abstract. — Experimentally observed configurations of the integration of glide dislocations into a $\Sigma = 9$ boundary are explained in analogy to cross-slip in the bulk. Crystallographically possible dissociations of the bulk dislocations into complete or imperfect dislocations of the DSC lattice are discussed. The energetically most favorable configurations serve as activated intermediary steps in thermal activation involving both glide and climb. Thermal activation blocks 60° dislocations at the boundary, but helps screw dislocations to traverse it.

1. Transmission of slip across grain boundaries.

1.1 THE PROBLEM. — Hirth [1] was the first to consider the necessity and possibility of slip across grain-boundaries. Before a dislocation gliding in one grain can glide into the other grain, it has to cross the boundary between. The problem of transmission of slip is thus a twofold one : first the glide dislocation has to enter the boundary, then it has to leave it again. Since Hirth's paper the subject has advanced considerably, mainly because of the work on crystallographically well defined boundaries. In particular, conventional electron microscopy [2], synchrotron topography, 1 MeV *in situ* experiments [3, 4] and high resolution electron microscopy [5, 6] on $\Sigma = 9$ silicon bicrystals greatly improved the understanding of the behaviour of glide dislocations near or « at » the boundary (for a review see [7]). Though discussed [8] but still unsolved is the problem of actual incorporation into and transmission across the boundary of the dissociated dislocations. Apparently this process does not happen

spontaneously, and although macroscopically necessary and observed, still eludes understanding on a crystallographic and energetic level.

In this paper we propose two new ideas : firstly we invoke (and give evidence for) the existence of grain-boundary partials, and secondly, we invoke thermal activation of three-dimensional critical configurations. When dissociation of the in-coming dislocation occurs within the boundary, transmission of slip is impeded. When dissociation occurs only on the glide planes of the other grain, slip into the other grain is easy.

1.2 EXPERIMENTAL DETAILS. — $\Sigma = 9$ bicrystals were obtained by the Czochralski method. Both the grains and the GB plane were dislocation-free. The GB plane was $(\bar{1}2\bar{2})_{\mathrm{I}}$ or $(12\bar{2})_{\mathrm{II}}$ (subscripts I and II are for crystal I and crystal II respectively), the common tilt axis was [011] and the tilt angle was 38.94°.

The stress experiments were performed by Jacques and George at the Ecole des Mines de Nancy, France, the deformation conditions being as described in an earlier paper [9]. The compression stress was applied along the $[\bar{2}6, 7, 20]_{\mathrm{I}}$ axis, equivalent to the $[\bar{2}6, 20, 7]_{\mathrm{II}}$ axis and was contained in the GB plane. The deformation condition was a single slip condition in both crystals. The deformation was stopped in the yield region and samples cooled down under load in order to freeze-in the dislocation-GB configurations. In the traction tests the stress axis was $[41\bar{1}]_{\mathrm{I}}$, equivalent to $[4\bar{1}1]_{\mathrm{II}}$. The deformation conditions are summarized in table I.

Table I. — *The deformation conditions of the observed samples are summarized in this table. T : temperature in K, ε : strain in %, $\dot{\varepsilon}$: strain rate in* s^{-1}. *The compression tests and the tension tests are indicated by (c) and (t) respectively.*

T (K)	ε(%)			$\dot{\varepsilon}$ (s^{-1})
870		1.2(c)		10^{-6}
970	0.5(c)			10^{-6}
1 020	0.4(c)	1.3(t)		5×10^{-6}
1 120	0.3(c)	1.7(c)		5×10^{-6}
1 220			6.8(c)	5×10^{-6}
1 470		1.5(c)		5×10^{-6}

After deformation the samples were mechanically cut and polished to a thickness of 70 μm. Discs 3 mm in diameter were then extracted by ultrasonic grinding, and ion-thinned. A final chemical polishing at 0 °C revealed the grains and GB dislocations. Rapid ion-thinning (15 mn) and chemical polishing were then undertaken between successive observations in order to explore a maximum length of GB.

The samples were observed with a JEOL 200 CX electron microscope equipped with an ultra-high-resolution pole-piece ($C_s = 1.05$ mm). The common [011] axis of the bicrystal was parallel to the electron beam.

The only dislocations studied were those lying along the [011] axis. They were viewed end-on in the microscope.

Owing to the choice of deformation axis in the compression tests, the activated slip system with the highest Schmid factor ($s = 0.467$) was the most favourable one for HREM

observations : $(\bar{1}\bar{1}1)_I$, $[\bar{1}10]_I$ or $(1\bar{1}1)_{II}$, $[10\bar{1}]_{II}$. Consequently, on these primary planes, 60° dislocations were observed edge-on. Another slip system ($s = 0.382$) was detected on the same planes, which led to screw dislocations observed edge-on too : $(\bar{1}\bar{1}1)_I$, $[011]_I$ or $(1\bar{1}1)_{II}$, $[0\bar{1}\bar{1}]_{II}$. An additional slip system ($s = 0.217$) could also be observed : $(\bar{1}1\bar{1})_I$, $[10\bar{1}]_I$ or $(11\bar{1})_{II}$, $[1\bar{1}0]_{II}$. In the tension tests, the Schmid factor of the slip system inducing 60° dislocations (line 011) on the primary planes is 0.408, whereas it is 0.226 on the additional planes. The slip systems inducing screw dislocations aligned along 011 are not activated in tension.

2. Grain-boundary partial dislocations.

2.1 DSC LATTICE. — A grain-boundary dislocation (GBD) in a coincidence grain boundary (GB) has a Burgers vector belonging to the associated DSC lattice [10]. The sign for the Burgers vector is given by the SF/RH convention on the open circuit around the dislocation pointing into the paper as given by Hirth and Lothe [11]. The Burgers vector of a GBD and the height of the associated GB step are measured following the method described by King and Smith [12]. It has to be noticed that the GB step connected with a given GBD Burgers vector has a precisely determined height even if several values can exit. The characterization of the defects in the grain and in the boundary is based on the fact that the Burgers vectors and the associated step heights are conservative.

Every point of the f.c.c. Bravais lattice of silicon is a point of the DSC lattice, but not *vice versa*. The DSC lattice associated with the $\Sigma = 9$ is a body centered one with a Cartesian basis consisting of :

$$b_c = \frac{a}{9}[\bar{1}2\bar{2}]_I = \frac{a}{9}[12\bar{2}]_{II}, \; b_g = \frac{a}{18}[\bar{4}\bar{1}1]_I = \frac{a}{18}[\bar{4}1\bar{1}]_{II}$$

and

$$2s = \frac{a}{2}[011]_I = \frac{a}{2}[011]_{II}.$$

The elementary dislocations within this lattice are b_c, b_g and $b_{30}^1 = \frac{1}{2}(b_c + b_g + 2s)$ (Fig. 1a). b_c and $-b_c$ are not associated with a GB step unlike the other GBD's. The GB step heights associated respectively with b_g and $-b_g$ are $-h_0$ and $+h_0 (h_0 = a/3)$ [5]. There are 4 distinct projections of the 30° GBD Burgers vector : b_{30}^1, b_{30}^2, b_{30}^3, b_{30}^4. Each b_{30} is found associated with a step of two possible heights : b_{30}^1 with $h = 1.75\, h_0$ or $-2.75\, h_0$, b_{30}^2 with $h = -1.75\, h_0$ or $2.75\, h_0$, b_{30}^3 with $-1.75\, h_0$ or $+2.75\, h_0$ and b_{30}^4 with $h = 1.75\, h_0$ or $-2.75\, h_0$. Due to the GB symmetry, only four different structures exist : b_{30}^1 with $h = 1.75\, h_0$ and $-2.75\, h_0$ and b_{30}^3 with $h = -1.75\, h_0$ and $2.75\, h_0$, the others can be deduced by a mirror symmetry with respect to the GB plane. The screw component of the Burgers vector will not be given in the following owing to the fact that by HREM, which only gives the projection, it is not observable. However, at least in the compression tests, the stress conditions would permit us to deduce the sign of the screw component of the observed dislocations. On both sides of a DSC dislocation the GB structure is unchanged. Within the grain-boundary a network of the three elementary dislocations can be formed.

2.2 DSC PARTIAL DISLOCATIONS. — In our observations, two other types of GB dislocations were detected that we will define as « imperfect » or « partial » dislocations.

i) The first type is a dislocation located in the GB but connected with another grain partial dislocation through a stacking fault extended in the grain.

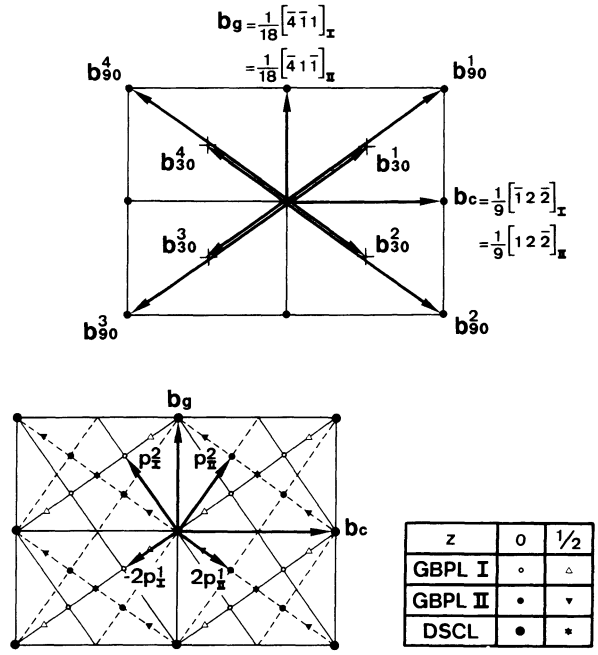

Fig. 1. — a) $\Sigma = 9$ DSC lattice projection along [011]. Definition of the terminology used in the text (●) lattice point at level $z = 0$, and + lattice point at level $z = \pm \frac{a}{4}$ [011]. Grain I is on the left hand side of the vertical axis, grain II on the right hand side. b) Projection along the [011] axis of the two lattices GBPL1 and GBPL2 that define the partial vectors of the DSC lattice : $2p^1_I = a/18\,[\bar{2}1\bar{1}]_I$, $p^2_I = a/9[\bar{1}\bar{1}1]_I$, $2p^1_{II} = a/18[21\bar{1}]_{II}$, $p^2_{II} = a/9[\bar{1}1\bar{1}]_{II}$.

If the stacking fault (SF) lies on the primary plane, we observed an « imperfect » GBD whose Burgers vector is a DSC vector. However, the structure of the GB dislocattion bonded to a grain SF is not the same as the one of the isolated GBD : see for instance in figure 2a the b_c dislocation resulting from the decomposition of the 90° partial incoming on the primary planes (DSC vector) into a glissile perfect b_g GBD (DSC vector) and an imperfect b_c dislocation. Futhermore this b_c imperfect GB defect (DSC vector) has an associated step whose height is $h = 1.5\,h_0$, $(h_0 = a/3)$, whereas the isolated perfect GB b_c is characterized by a well defined structural unit (a boat-shaped six-atom ring called T by Bourret and Bacmann [13] and has no associated step (Fig. 2b).

If the SF lies on the additional planes, we observed an « imperfect » dislocation whose Burgers vector does not belong to the DSCL : see in figure 2c the observation of the p^1_{II}.

ii) The second type is a dislocation located in the GB but connected with another GB dislocation through a « grain-boundary SF » (GBSF) (Fig. 2d). The total Burgers vector of the global configuration is a DSCL vector like any GBD Burgers vector. These defects could be defined as « partial » GB dislocations. In the case of the $\Sigma = 9$ GB, this GBSF can be described as a combination of boat-shaped six atom rings on the additional plane close to the five-seven atom rings structural units of the $\Sigma = 9$ GB. This GBSF never extends over more than one period of the GB leading to the idea that this structure is of high energy.

The previous configurations were described in terms of dissociation in analogy to the dissociation in the bulk. Therefore, we used the words « GBSF » and « partials ». However,

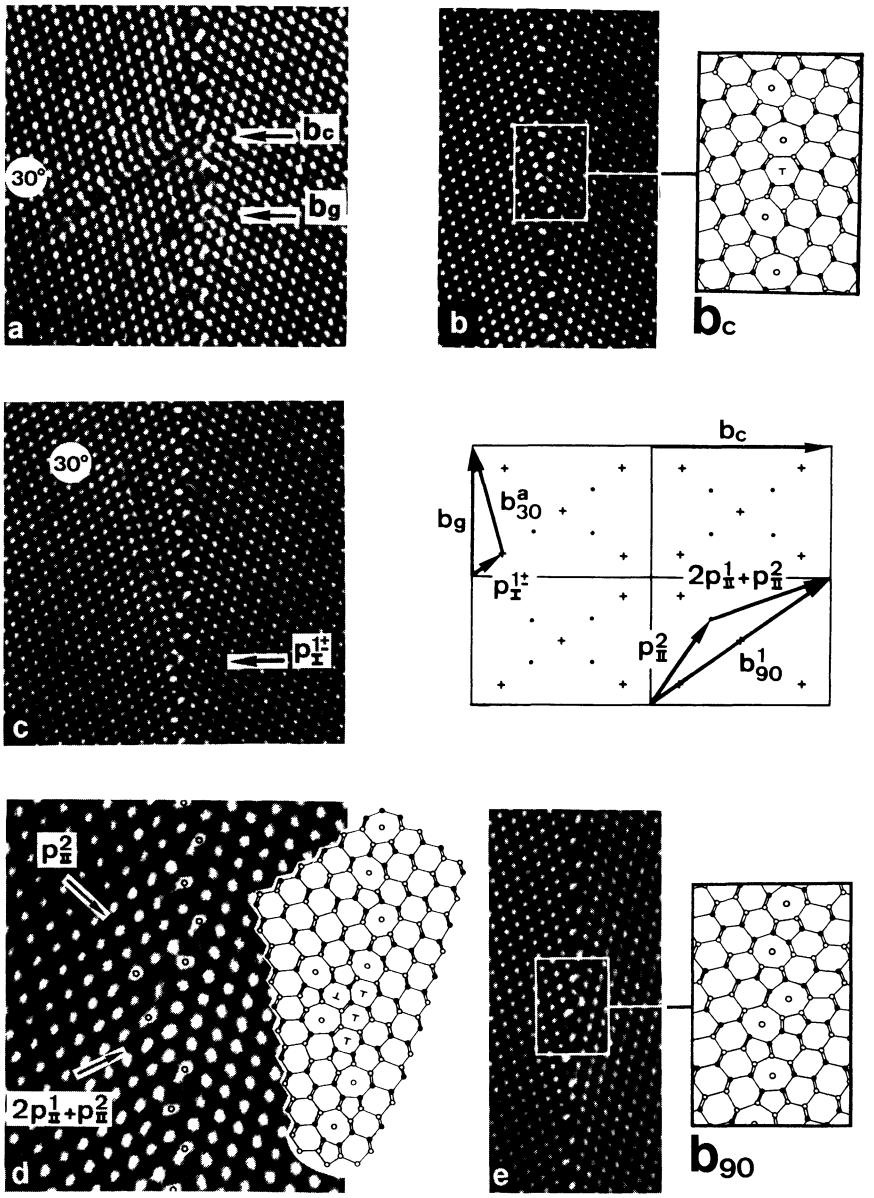

Fig. 2. — a) Observation of the « imperfect » b_c GBD connected with a GBSF in grain I. The b_c vector is a DSC perfect vector (micrograph M. Elkajbaji) however the step height is $h = +1.5\,h_0$ whereas the perfect b_c GBD (b) is isolated in the GB and characterized by the T boat-shaped six-atom ring ($h = 0$). c) Observation of the $p_I^{1\mp}$ grain-boundary partial dislocation. Because of the projection, only the edge component $p_I^1 = \frac{a}{36}[\bar{2}1\bar{1}]$ can be seen, the screw component $\pm s = \frac{a}{4}[011]$ remains invisible. The partial p_I^{1+} (or p_I^{1-}) borders an intrinsic stacking fault that extends into grain I. d) Observation of a p_{II}^2 grain-boundary partial dislocation. The partial borders a γ' « stacking fault » of the $\Sigma = 9$ grain boundary, terminated on the other side by a $(p_{II}^2 + 2\,p_{II}^2)$ imperfect dislocation. The total Burgers vector is b_{90}^1. This configuration has to be compared with the non dissociated configuration (e) of the same b_{90}^1 (micrographs with black atoms and O on the seven atom rings).

this idea and its structural and energetical consequences have to be clarified, but will not be detailed in this paper.

The concept of DSC partials was already introduced to describe the defects separating two structurally distinct (but energetically equivalent) parts of the same Σ GB or to define the linear jonctions between facets [14, 15, 16]. In our case, the concept of « partials » is slightly different : as mentioned the energy of the GBSF might be certainly higher than the energy of the initial $\Sigma = 9$ and futhermore the structure of the GBSF is completely coupled to one or the other adjacent grain, *via* the boat six-atom rings.

The « partial » GBD Burgers vector could be described with the help of the two orthogonal bases consisting of $2\,p_{\mathrm{I}}^1 = \frac{a}{18}\,[\bar{2}1\bar{1}]_{\mathrm{I}}$, $p_{\mathrm{I}}^2 = \frac{a}{9}\,[\bar{1}\bar{1}1]_{\mathrm{I}}$ and $2\,s$, or $2\,p_{\mathrm{II}}^1 = \frac{a}{18}\,[21\bar{1}]_{\mathrm{II}}$, $p_{\mathrm{II}}^2 = \frac{a}{9}\,[\bar{1}1\bar{1}]_{\mathrm{II}}$ and $2\,s$, both being centered on the faces with normal p^2 (i.e. they have additional points at $(p^1 + s)$, see Fig. 1b). Physically realized are the partial dislocations $p^{1-} = p^1 + s$, $p^{1+} = p^1 - s$ and p^2. In our images, which are projections in the s-direction, only the components p^1 and p^2 are observable, and have actually been observed (Fig. 2c, d).

3. Thermal activation.

Although our observations are restricted to two-dimensional configurations, the possibility that the actual mechanism of absorption of the dislocations by the grain-boundary is not a two-dimensional but a three-dimensional process, cannot be excluded. On the contrary, it seems even probable that similar to cross slip or climb in the bulk, thermally activated configurations are involved. However, the activated configurations in the boundary are substantially different from the ones envisaged for bulk cross slip. In the cross slip model of Schoeck *et al.* [17, 18] a totally constricted configuration over a finite length is invoked which moves off into the cross-slip plane by dissociating. In the analogous grain-boundary cases, some residue must be left behind where the constricted dislocation was, because the slip vectors in grain I and in the boundary are not the same. In the cross slip model of Friedel and Escaig [19, 20] no total constriction exists over any finite length, but a constricted point dissociates into the cross-slip plane. A model of cross-slip from a single partial, without constriction was proposed first by Fleischer [21]. In the analogous grain boundary case the dislocation rests on its slip plane, but a point of the leading partial expands into a faulted loop in the grain boundary plane. Unlike in cross-slip, the fact that the possible Burgers vectors of the grain-boundary dislocations can do work not only by glide, but also by climb [22], influences merely the work term in the exponent of the Arrhenius expression [23].

3.1 Integration of 60° dislocations.

3.1.1. *Tension with glide on the primary plane.* — The 60° dislocation arrives on the $(\bar{1}\bar{1}1)_{\mathrm{I}}$ plane in grain I, the 30° partial in front and the 90° partial trailing behind. The integration of the complete 60°D in the GB would have left a GB defect characterized by a total Burgers vector b_{60}^3 with an associated height $h = -0.75\,h_0$. The applied stress, possibly even augmented because the dislocation under consideration might be the first one of a pile-up, presses the leading 30° partial (though b_{30}^3 = DSC vector) against the boundary. If the activation follows the upper path of figure 3, a loop of a complete GBD $-b_{\mathrm{g}}(h = -h_0)$, is emitted in the boundary plane, leaving a $b_{30}^4 = \frac{a}{6}\,[\bar{1}12]_{\mathrm{II}}$ imperfect GBD at the intersection with an associated step whose height is $h = -0.75\,h_0$, whereas the perfect b_{30}^4 GBD has an associated step whose height is either $1.75\,h_0$ or $-2.75\,h_0$ [5]. Since $-b_{\mathrm{g}}$ is glissile in the boundary, the loop size increases under the boundary traction stemming from the pile-up,

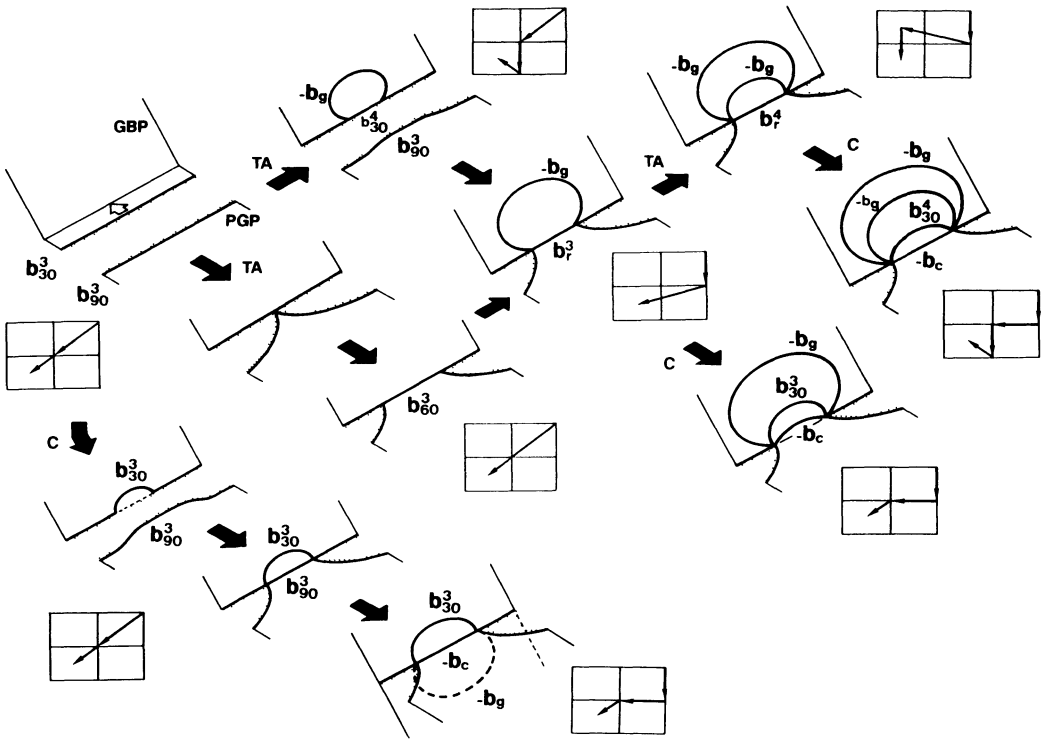

Fig. 3. — The integration into the grain boundary plane (GBP) of a 60° dislocation in tension, glide on the primary plane (PGP) of grain I, which is $(\bar{1}\bar{1}1)_I$. In the small rectangular insert the various decompositions of the Burgers vectors are shown with respect to grain I. The upper path illustrates the thermally actived (TA) glide model of Friedel and Escaig, the middle path shows the thermally activated glide model of Seeger and Schoeck. Both lead to the b^3_r constricted configuration. In the lower path, supersaturation of point defects allows climb (C) of the leading partial (which in this favorable case belongs to the DSC lattice) in the grain boundary. The integration and decomposition of the trailing partial follows spontaneously. This path leads to a b^3_r decomposed into b^3_{30} and $-b_c$.

whereas the applied stress is inactive, its traction being zero in the boundary. We take this to be the configuration of highest energy, i.e. the activated one. The b^4_{30} GBD and the 90° partial are almost perpendicular ; then, the stacking fault in between and the pile-up stress pull them together into a « constricted » $b^3_r(h = -1.75\,h_0)$, (Fig. 4a). Because of the energy gain the b^3_r line gets spontaneously longer. Either it remains constricted or it decomposes by climb into DSC dislocations : $-b_c = \frac{a}{9}[1\bar{2}2]_I$ $(h = 0)$ plus $b^3_{30} = \frac{a}{6}[112]_I$ $(h = -1.75\,h_0)$, (Fig. 4b). Under another thermal activation the $b^3_r(h = -1.75\,h_0)$ can form a $b^4_r(h = -2.75\,h_0)$ by splitting off another $-b_g$ (or receiving a $+b_g$ already present in the boundary). Under our experimental conditions (deformation at 1020 K) the completely constricted $b^3_r(h = -1.75\,h_0)$ or $b^4_r(h = -2.75\,h_0)$ have never been observed. Instead we found closely dissociated forms : figure 4a shows the dissociated form of b^3_r into $-(p^2 + 2p^1 + p^{1\pm})_{II}$ plus $-(2p^1 + p^2)_{II}$. The b^4_r is dissociated into $-4p^1_{II}$ plus $(-p^2 - 2p^1 - p^{1-})_{II}$, see figure 4c. If climb is available, the b^4_r can decompose further into a $b^4_{30}(h = -2.75\,h_0)$ plus $-b_c$, see figure 4d. The measurement of each partial Burgers vector, using the King and Smith [12] method was only possible in the case of the b^4_r dissociation. The partials of b^3_r (Fig. 4a) were

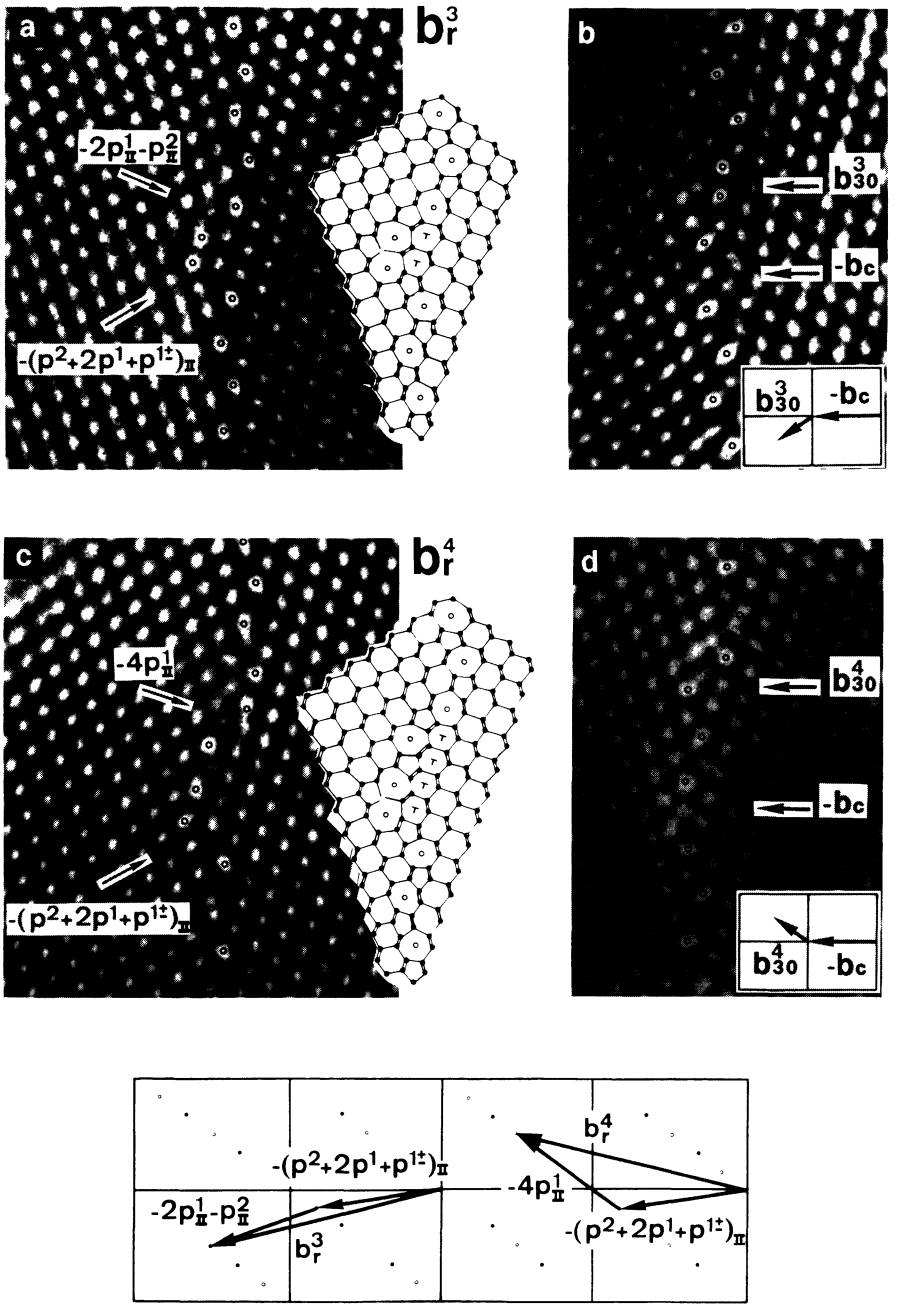

Fig. 4. — Residues left by a 60° dislocation in tension (1020 K, 1.3 %). (a) and c) show the b_r^2 and b_r^4 residual dislocations left after integration of the 60° dislocation (upper and middle paths in Fig. 3). They are slightly dissociated into DSC partials (lower scheme). The necessary stacking fault appears as a bulk stacking fault (T units) attached to the grain boundary on one or the other additional (111) plane. (b) and (d) Elementary DSC dislocations left after the decomposition of b_r^3 and b_r^4 respectively : the b_{30}^3 $(h = -1.75\, h_0)$ and $-b_c(h = 0)$ in (b), and the $b_{30}^4(h = -2.75\, h_0)$ and $-b_c$ in (d) (micrographs with black atoms and O on the seven atom rings).

deduced *a posteriori* by comparing the structural models of the dissociated b_r^3 and b_r^4 proposed in figure 4a and c. If the activation follows the middle path of figure 3, the trailing 90° partial $b_{90} = \frac{1}{6}[2\bar{1}1]_I$ follows spontaneously to produce a constriction at one point. This constriction is extended and this complete 60° dislocation ($h = -0.75\,h_0$) decomposes spontaneously into $-b_g(h = h_0)$ plus $b_r^3(h = -1.75\,h_0)$ reaching the configuration discussed before.

In principle, if one allows climb (the existence of which has been shown experimentally in the grains [24]) during the last stages of the upper and middle paths of figure 3, one has to allow for the possibility that the leading b_{30}^3 climbs immediately in the boundary, until the b_{90} partial is pulled into the boundary by the stacking fault. The result of the spontaneous decomposition of the b_{90}^3 into $-b_c$ plus $-b_g$ leads to the same configuration as before.

3.1.2 *Compression with glide on the primary plane.* — The 60° dislocation arrives again on the $(\bar{1}\bar{1}1)_I$ plane of grain I, with the 90° partial in front and the 30° partial trailing behind. The integration of the complete 60 °D would have left a GB defect characterized by a Burgers vector b_{60}^1 associated with a GB step whose height is $h = +0.75\,h_0$. The b_{90} decomposes into the perfect GBD $b_g(h = -h_0)$ plus the « imperfect » GBD $b_c(h = 1.5\,h_0)$, the former doing work under internal stresses by gliding in the boundary. If the upper path of figure 5 is followed, a loop of b_g is formed (doing work), leaving a b_{90}^2 imperfect edge behind. This GBD

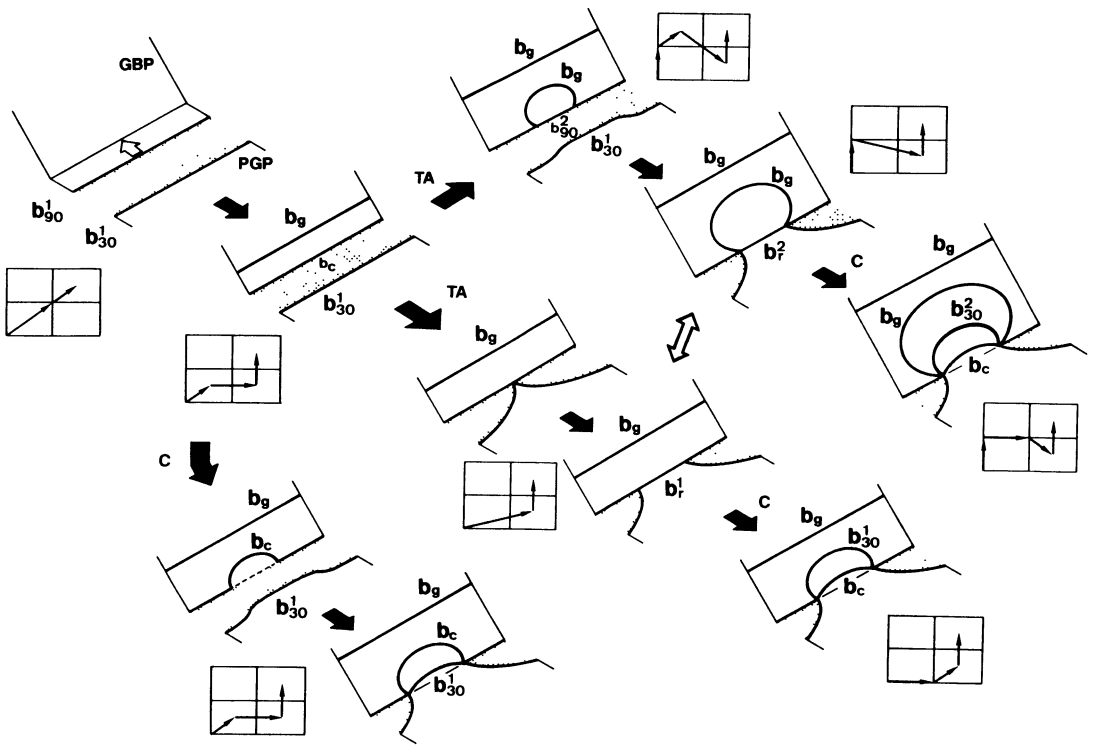

Fig. 5. — The integration of a 60° dislocation in compression, glide on primary planes (PGP) of grain I which is $(\bar{1}\bar{1}1)_I$. In the small rectangular inserts the various decompositions of the Burgers vector are shown with respect to grain I. As in figure 3, three possible paths are presented. The upper and middle ones show thermally activated (TA) glide mechanisms. The lower one takes place when climb(C) occurs. Residues are the constricted b_r^1 and b_r^2 dislocations, and the decomposed b_r^1, respectively.

is almost perpendicular to the 30° partial left behind and the stacking fault combines them to a constricted b_r^2. Either this one remains or, if climb is possible, decomposes into $b_{30}^2 + b_c$. If the middle path of figure 5 is followed, the 30° trailing approaches the b_c by thermal activation to give a constricted b_r^1. The completely constricted or slightly dissociated configurations of b_r^1 and b_r^2 have never been detected even at 970 K. They were always found decomposed by climb in either :

$$b_r^1(h = 1.75\, h_0) \rightarrow b_{90}^1(h = -h_0) + b_{30}^2(h = 2.75\, h_0)\ [1] \quad \text{(Fig. 6a)}$$

or

$$b_r^1(h = 1.75\, h_0) \rightarrow b_c(h = 0) + b_{30}^1(h = 1.75\, h_0) \quad \text{(Fig. 6c)}\ .$$

On the other h and

$$b_r^2(h = 2.75\, h_0) \rightarrow b_c(h = 0) + b_{30}^2(h = 2.75\, h_0) \quad \text{(Fig. 6d)}\ .$$

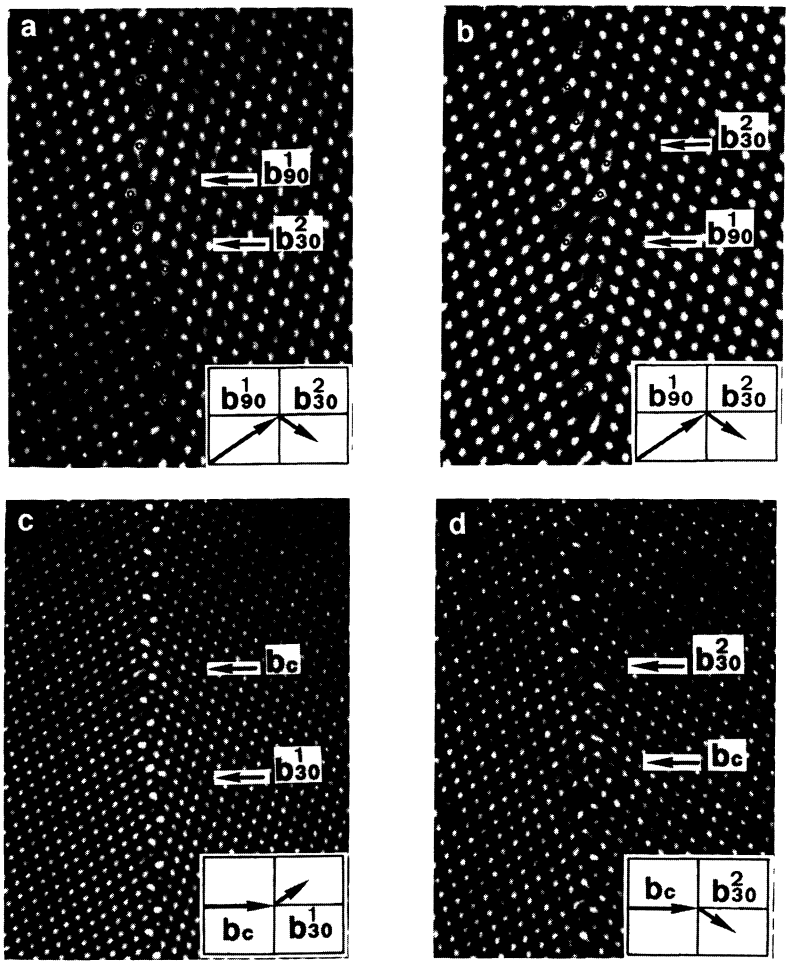

Fig. 6. — The integration of a 60° dislocation in compession, glide on primary planes. (a) and (b) correspond to the b_r^1 in two different decomposed core configurations where the DSC dislocations b_{90}^1 and b_{30}^2 are recognizable. In (a) b_{90}^1 is in a compact form unlike in (b) where it is dissociated (micrograph M. Elkajbaji). (c) and (d) show the complete decomposition of b_r^1 and b_r^2 into $b_{30}^1 + b_c$ and $b_{30}^2 + b_c$. Deformation conditions (a) and (c) $T = 1120$ K, $\varepsilon = 1.7$ %, (b) and (d) $T = 1120$ K, $\varepsilon = 0.3$ % (micrograph with black atoms and O on the seven atom rings).

These final results all involved climb. In the reaction [1], the b^1_{90} DSC GBD is sometimes found in a slightly dissociated form :

$$b^1_{90}(h = -h_0) \rightarrow p^2_{II} \cdots \text{GBSF} \cdots + (2p^1_{II} + p^2_{II}) \quad \text{(Fig. 6b)} .$$

The lower path of figure 5 illustrates the direct climb integration of the b_c DSC GBD into the boundary. This mechanism leaves an « imperfect » pure step ($h = 1.5\, h_0$) in the GB. The 30° trailing partial could then enter spontaneously.

3.1.3 *Tension with glide on the additional plane.* — The 60° dislocation arrives on the $(\bar{1}1\bar{1})_I$ plane of grain I, with the 30° partial $b^a_{30}(I)$ in front and the 90° partial trailing behind. These partials do not belong to the DSC lattice. The integration of the complete 60 °D would have left a GBD whose Burgers vector would have been the initial 60 °D Burgers vector and whose associated step height would have been $h = +0.25\, h_0$. By thermal activation the 30° partial $b^a_{30}(I) = -(p^1_I + p^2_I)$ decomposes into $-b_g$ plus a partial p^{1+}_I (Fig. 7 upper path). The loop of the $-b_g$ expands. Recombination of the p^{1+}_I with the trailing $b^a_{90}(I) = (-2p^1_I - 4p^2_I)$ is energetically favourable to form a $b^2_p(h = -0.75\, h_0)$ constricted dislocation belonging to the DSCL. This one decomposes spontaneously into another $-b_g$ plus a remaining $b^2_{30}(h = -1.75\, h_0)$. However, like in the other cases, spontaneous constriction over a certain

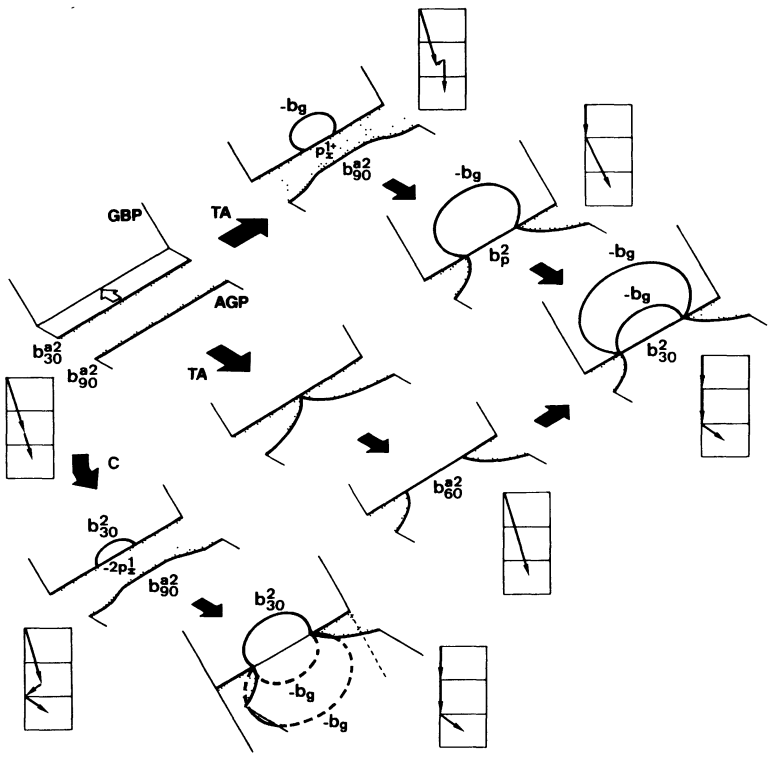

Fig. 7. — The integration of a 60° dislocation in tension, glide on additional planes(AGP) of grain I which is $(1\bar{1}1)_I$. In the small rectangular inserts the decompositions of the Burgers vector are shown with respect to grain I. As in the other cases three paths are given. The two upper ones require glide only, but the lower one requires climb (C). In this case the leading partial must dissociate into a DSC partial $-2p^1_I$ plus b^2_{30}. In order to have a more legible pattern, the angle between the additional plane and the GB plane is not correctly reproduced.

length cannot be excluded, and the resulting $b^{a}_{60}(I)$ (never observed) could decompose into either one of the previous configurations. Unlike in the previous case (lower path of 3.1.2), the leading partial cannot climb on its whole in the boundary. Moreover, a further climb decomposition could lead to b^{2}_{30} plus $(-2\,p^{1}_{I})$. The stacking fault then repels the trailing partial spontaneously. The boundary residual is $-2\,b_g$ and can immediately glide off in the boundary. The three paths lead to the same $b^{2}_{30}(h = -1.75\,h_0)$ residual dislocation. As shown in table I, only one series of samples deformed in tension was studied and furthermore, as mentioned in § 1.2, the Schmid factor of this slip system is relatively low and consequently the number of dislocations gliding on the additional planes is extremely low. Thus we found only one GB defect unambiguously related to the above described mechanism : this GBD is completely isolated on a wide length of perfect GB, its Burgers vector is $b^{1}_{30}(h = -2.75\,h_0)$ and this defect results from the interaction of the initial $b^{2}_{30}(h = -1.75\,h_0)$ with a glissile $b_g(h = -h_0)$ GBD. This b^{1}_{30} arises unlikely from the direct decomposition $(b^{1}_{30} - 3\,b_g)$ of the initial 60 °D $(h = 0.25\,h_0)$ coming on the additional plane.

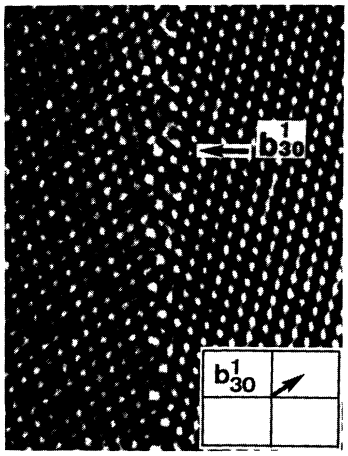

Fig. 8. — The final results of the different paths of the integration of a 60 °D in tension on additional planes are the same : only one $b^{2}_{30}(h = -1.75\,h_0)$ has to be found in the boundary or one $b^{1}_{30}(h = -2.75\,h_0)$ which is shown in the picture and which results from the interaction between b^{2}_{30} and another glissile $b_g(T = 1020\ \text{K}, \varepsilon = 1.3\%)$.

3.1.4 *Compression with glide on the additional plane.* — The 90° partial arrives first and decomposes by thermal activation into two $-b_g$ dislocations plus a remaining partial $(-2\,p^{1}_{I})$ (Fig. 9). Since the two $-b_g$ do work in the boundary by glide, and since the two reaction products are almost perpendicular to each other, this process might actually proceed without thermal activation. Subsequently the $(-2\,p^{1}_{I})$ and the 30° trailing attract each other spontaneously to form a $b^{4}_{30}(h = 1.75\,h_0)$ as observed in figure 10. The same result might be reached by thermally activating a total constriction into a $b^{a}_{60}(I)$ $(h = -0.25\,h_0) = 2\,b_g + b^{4}_{30}(h = 1.75\,h_0)$. The leading partial cannot climb on its whole in the GB. A combination of b_g emission and of climb decomposition into partials (lower path Fig. 9) leads to the same b^{4}_{30} residue.

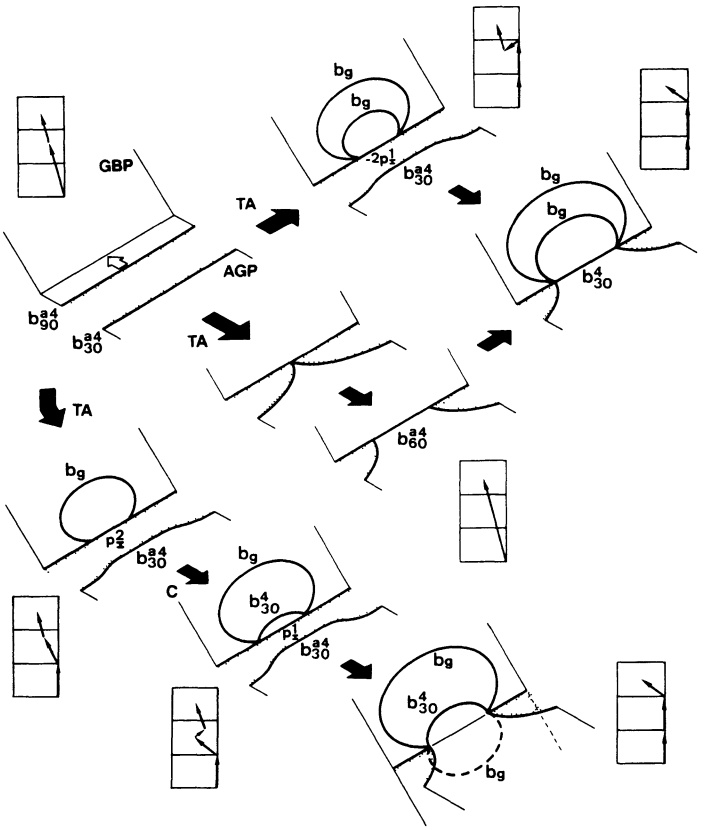

Fig. 9. — The integration of a 60° dislocation in compression, glide on additional planes(AGP) of grain I. In the small rectangular inserts the Burgers vector decompositions are shown with respect to grain I. Three paths analogous to the three paths of figure 7 are drawn. They all give the same b_{30}^{4} residue under glide or climb integration (the remark in Fig. 7 about the angle between the additional planes and the GB plane is valid here as well).

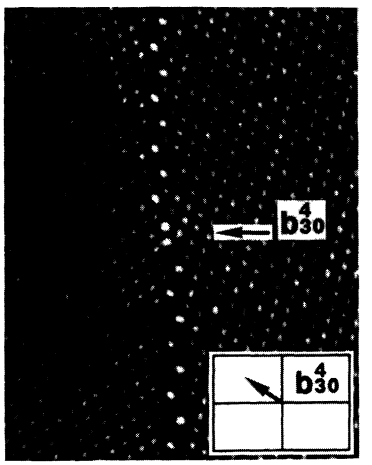

Fig. 10. — The integration of a 60° dislocation in compression, glide on additional planes. The b_{30}^{4} is found completely isolated and can only be the result of the decomposition shown in figure 9. The step height is $+ 1.75\, h_0$ (black atoms) ($T = 970$ K, $\varepsilon = 0.5$ %).

3.2 A SCREW DISLOCATION ON ANY PLANE UNDER TENSION OR COMPRESSION. — This is the simplest case. Like in cross-slip in the bulk, the two Shockley partials could recombine to form a constricted screw by thermal activation, and dissociate again on one or the other glide plane of the other grain. Dissociation of the constricted screw that produces b_g glissile dislocations in the boundary is highly improbable, nor is it probable by using the partials of section 2. If the screw remains dissociated, the emission of a b_g from the leading 30° partial like in the case figure 3 (upper path) would lead to an even more unlikely configuration where the trailing partial would be repelled at a higher distance than before. If climb is available, the constricted screw dislocation could dissociate and consequently be stopped at the boundary. Figure 11 shows a configuration without any global Burgers vector which might be the projection of a screw dislocation dissociated in the GB plane. As the screw component is invisible two structures could be proposed (Fig. 11b, c). In the first case the core of two 30° GB dislocations is recognizable : the screw is decomposed by climb absorbing two interstitials. In the second case (c) a completely reconstructed defect could be imagined using T units : this residue, which also consumed two interstitials, might be left in the GB after the reemission of the screw dislocation from the previous rearranged compact configuration. Owing to the stability of the initial $\Sigma = 9$ GB a direct absorption of interstitials inducing a structural change could be dismissed. We could not decide in favour of either one or the other model. Nevertheless, it remains valid that if large climb occurs, the two initial b_{30} would climb over a larger distance impeding the transmission of the screw. If climb is not available, having no other choice, the screw dislocation traverses the boundary, presumably with an activation energy very similar to cross slip in the bulk. Baillin *et al.* [3] have indeed seen by *in situ* HVEM electron microscopy screws traversing the boundary. At low temperature (T lower than 970 K), using high resolution microscopy, we never observed any GB residue stemming from screws. This seems to confirm their findings.

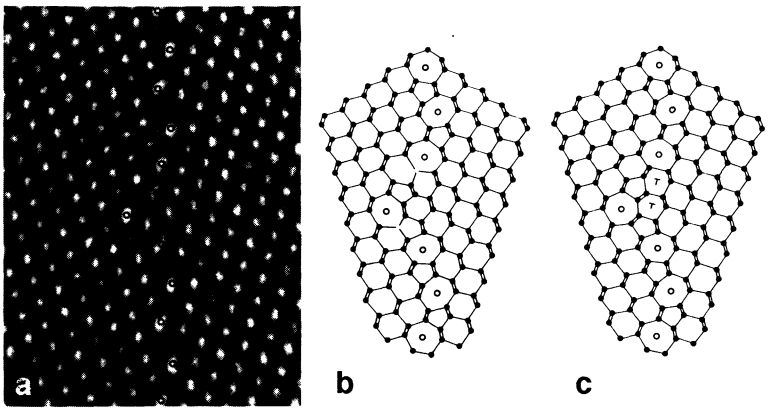

Fig. 11. — Observation of a screw dislocation completely integrated in the GB but decomposed into two 30° DSC dislocations. The total Burgers vector is null in projection whereas the core of both 30° DSC dislocations can be recognized (micrograph M. Elkajbaji). Compression 1.7 %, $T = 1120$ K (O on the seven atom rings).

4. Discussion.

The reader might be disappointed that we offer no preference for the upper or lower path of figures 3, 5, 7, 9 (in 3.1.1, in 3.1.2, in 3.2.1, in 3.2.2). The upper path, is in fact a mechanism deduced from a combination of both the Fleischer and the Friedel-Escaig models, in the sense

that a point of the leading partial decomposes into a perfect loop in the GB plane. The lower path is a modified version of the Seeger-Schoeck mechanism in the bulk. For the bulk, Bonneville, Escaig and Martin [25] offered experimental evidence for the Friedel-Escaig mechanism. In the case of thermally activated integration of a gliding dislocation in the boundary, we feel that our experiments are insufficient to decide in favour of one or the other reaction path. Since the activated configuration is, in principle, directly not observable, a distinction between one or the other path can be made only from their macroscopically observable consequences, or from thorough and precise calculations of the type made by Püschl and Schoeck [26]. The activation rates depend explicitly on temperature and applied and internal stresses, therefore one or the other mechanism might be preferred. Furthermore, the observed « partial » DSC dislocations, leads to the idea that the structure of the core of the intermediate configurations plays certainly a major role and might determine the ways of éntrance.

Besides these subtleties, the idea of thermally activated entry is a simple one. Crystallographically the 60° dislocation cannot cross over directly by glide into the other grain. Nevertheless work can be done by splitting off a dislocation glissile in the boundary, and this work facilitates entry. Crystallographically the screw dislocation cannot dissociate by glide in the boundary, but work can only be done in grain II, which favours cross-slip.

If climb is available even more configurations within the boundary become available, and transmission becomes even less likely.

Although thermal activation makes slip into the boundary likely and slip into grain II unlikely, the latter is not totally impossible. Whenever a totally constricted segment exists in the boundary, one can force its decomposition into a glide loop in grain II plus some residue in the boundary by very high applied stresses — if thermal activation is available : this explanation might account for transmission of non screw dislocations as observed by Jacques, Baillin and George [27].

5. Conclusion.

This 60° dislocation can, and the screw dislocation cannot emit a b_g dislocation glissile in the boundary. Only under very high stresses the 60° dislocation can split off a dislocation glissile in grain II. Only by climb the screw dislocation partials can move in the boundary. Therefore the 60° dislocation is integrated in the boundary (but transmitted only under high stresses), and the screw dislocation traverses into grain II (but is integrated into the boundary under climb conditions). Thus thermal activation blocks 60° dislocations at the boundary, but helps screw dislocations to transverse it.

Acknowledgment.

The work was supported by the C.N.R.S. in France and the Austrian Academy of Sciences. H.O.K.K. acknowledges support by the Wiener Hochschuljubiläumsstiftung.

References

[1] HIRTH J. P., *Metall. Trans.* **A 3** (1972) 3047.
[2] MARTINEZ-HERNANDEZ M., KIRCHNER H. O. K., KORNER A., GEORGE A. and MICHEL J. P., *Philos. Mag.* **A 56** (1987) 641.
[3] BAILLIN X., PELISSIER J., BACMAN J. J., JACQUES A. and GEORGE A., *Philos. Mag. A.* **55** (1987) 143.
[4] JACQUES A., GEORGE A., BAILLIN X., BACMANN J. J., *Philos. Mag.* **A 55** (1987) 165.

[5] ELKAJBAJI M. and THIBAULT-DESSEAUX J., *Philos. Mag.* **A 58** (1988) 325.
[6] THIBAULT-DESSEAUX J., PUTAUX J. L., JACQUES A., ELKAJBAJI M., Interfacial Structure, Properties and Design, *MRS Ser.* **122** (1988) 293.
[7] GEORGE A., *Rev. Phys. Appl.* **23** (1988) 479.
[8] KING A. H., CHEN F., *Mat. Sci. Eng.* **66** (1984) 227.
[9] ELKAJBAJI M., THIBAULT-DESSEAUX J., MARTINEZ-HERNANDEZ, JACQUES A., GEORGE A., *Rev. Phys. Appl.* **22** (1987) 569.
[10] BOLLMANN W., Crystal defects and crystalline interface (Springer Verlag) 1970.
[11] HIRTH J., LOTHE J., Theory of Dislocations (McGraw-Hill) 1968, p. 21.
[12] KING A. H., SMITH D. A., *Acta Cryst.* **A 36** (1980) 335.
[13] BOURRET A., BACMANN J. J., *Rev. Phys. Appl.* **22** (1987) 563.
[14] SCHOBER T., BALLUFFI R., *Philos. Mag.* **21** (1970) 109.
[15] POND R., *Proc. R. Soc. London* **A 357** (1977) 471.
[16] BACMANN J. J., SYLVESTRE G., PETIT M., BOLMANN W., *Philos. Mag.* **A 43** (1981) 189.
[17] SCHOECK G., and SEEGER A., *Phil. Soc. London,* 340 (1955a) ; Report of the Bristol Conference on Defects in Crystalline Solids, London, Physical Society (1955b) p. 340.
[18] WOLF H., *Z. Naturforschung* **A 15** (1960) 180.
[19] FRIEDEL J., Dislocations and Mechanical Properties of Crystals, J. C. Fisher *et al.* Eds. (New York : Wiley) 1957, p. 330.
[20] ESCAIG B., *Phys. Stat. sol.* **28** (1968a) 463 ; *J. Phys.* **29** (1968b) 255 ; Dislocation Dynamics, Rosenfield, Hahn, Bemont, Jaffee Eds. (New York : McGraw Hill) 1968c p. 665 ; Thèse de Doctorat d'Etat, université de Paris, Centre d'Orsay, No A 382 (1968d).
[21] FLEISCHER R., *Acta Met.* **7** (1959) 134.
[22] THIBAULT J., ELKAJBAJI M., *J. Phys. Colloq. France* **49** (1988) C5-283.
[23] POIRIER J. P., *Rev. Phys. Appl.* **11** (1976) 731.
[24] THIBAULT-DESSEAUX J., PUTAUX J. L., KIRCHNER H. O. K., *Philos. Mag* (accepted).
[25] BONNEVILLE J., ESCAIG B. and MARTIN J. L., *Acta metall.* **36** (1988) 1989.
[26] PUSCHL W. and SCHOECK G., Strength of Metals and Alloys, Kettunen, Lepisto, Lehtonen Eds. (Pergamon Press) vol. I (1988) p. 239.
[27] JACQUES A., BAILLAIN X., GEORGE A., Strength of Metals and Alloys, Kettunen, Lepisto, Lehtonen Eds. (Pergamon Press) vol. I (1988) p. 245.